ISSN 0915-633X

NATIONAL INSTITUTE FOR FUSION SCIENCE

Particle Simulation Study of Dust Particle Dynamics in Sheaths

R. Smirnov, Y. Tomita, T. Takizuka, A. Takayama, Yu. Chutov

(Received - Oct. 9, 2003)

NIFS-784

Oct. 2003

RESEARCH REPORT
NIFS Series

TOKI, JAPAN

Particle Simulation Study of Dust Particle Dynamics in Sheaths

R. Smirnov[1], Y. Tomita[2], T. Takizuka[3], A. Takayama[2], Yu. Chutov[4]

[1] *The Graduate University for Advanced Studies, 322-6 Oroshi-cho, Toki 509-5292 Japan*

[2] *National Institute for Fusion Science, 322-6 Oroshi-cho, Toki 509-5292 Japan*

[3] *Naka Fusion Research Establishment, JAERI, Ibaraki 311-0193 Japan*

[4] *Taras Shevchenko Kiev University, Volodymyrska 64, Kiev 01033 Ukraine*

[This article is published in Contributions to Plasma Physics 2003.]

Particle Simulation Study of Dust Particle Dynamics in Sheaths

R. Smirnov[1], Y. Tomita[2], T. Takizuka[3], A. Takayama[2], and Yu. Chutov[4]

[1] The Graduate University for Advanced Studies, 322-6 Oroshi-cho, Toki 509-5292 Japan
[2] National Institute for Fusion Science, 322-6 Oroshi-cho, Toki 509-5292 Japan
[3] Naka Fusion Research Establishment, JAERI, Ibaraki 311-0193 Japan
[4] Taras Shevchenko Kiev University, Volodymyrska 64, Kiev 01033 Ukraine

Key words divertor plasma, dust particle, dynamics and charging, dust radius
PACS 52.40.Kh, 52.65.Cc, 52.65.Rr

Abstract
Dynamics of dust particles in a divertor plasma is simulated using numerical solutions of dust momentum and charging equations in an electrostatic sheath and an ionizing presheath, where an electrostatic force and a drag force due to absorption of plasma ions are taken into account. Spatial distributions of plasma parameters in a divertor are obtained with particle simulations including ionization by electron-impact. We found that the critical dust radius exists. Dust particles with a larger radius than this critical one are incapable to come off a divertor plate because the ion drag force is stronger compared to the electrostatic force. Control of the plate potential can suppress the dust motion from the plate. The radii of heavy dust particles are classified with respect to equilibrium positions. Considering dust particles started at the plate with radii smaller than the critical one, two types of dust motion were found. Dust particles with the first type of motion come back to the plate before approaching their equilibrium positions. The second type of motion is presented by smaller dust particles which oscillate around their equilibrium positions.

1 Introduction

Production of dust due to interaction of plasma with walls and divertor plates in fusion devices is going to be one of growing issues with expected long discharge time and high energy output. One of the main features of dust particles that differ them from other impurities is large self-consistent electric charge. Presence of such highly charged dust particles changes spatial potential distribution in divertor plasmas that modifies conditions for heat transmission [1, 2] and finally affects the boundary conditions for fusion plasma. So far, there are few direct experimental observations of dust particles in fusion devices, all of that concerned to dust collected from the inner vessel's walls after series of the discharges [3, 4]. However, there is a lack of data about dust particles properties during discharges. The questions of first interest are possible trajectories and density distributions of dust particles, their equilibrium positions and electric charges.

As known plasma near material walls, where dust particles usually created, forms electrically charged sheath and presheath. The potential drop in the presheath accelerates ions

toward the wall, so that the Bohm criterion can be satisfied at the sheath-presheath boundary [5]. A number of previous theoretical and numerical researches of dust motion in the sheath-presheath systems [6, 7, 8] considered fluid models of plasma or assumed constant charge of dust particles. In the present work, we study dynamics of dust particles in the divertor plasma that kinetically simulated with the particle code including the presheath formation by electron impact ionization. Therefore, the aim of the present research is investigation of motion of dust particles started from the divertor plate in plasma including both sheath and presheath, in particular investigation of the maximal distance that dust particles approach moving off the divertor plate.

2 Model

We consider the one-dimensional model of plasma facing the divertor plate under floating potential. The plasma consists of protons, electrons, and neutral hydrogen gas uniformly distributed with fixed density n_a and temperature T_a. The simulated system of the length L is bounded by the bulk plasma containing equilibrium electrons and ions with the constant densities $n_e = n_i = n_b$ and the temperatures T_{eb}, T_{ib}. The only elementary process accounted in the system is hydrogen ionization by electron impact that allows us to create the ionizing presheath. The divertor plate is assumed perfectly absorbing for electrons and ions, therefore no secondary emission and recycling considered. We do not consider the effect of a magnetic field on particles motion what implies, however, that the magnetic field which is perpendicular to the plate can be present in the system.

Simulation of plasma is carried out using 1D3V particles-in-cell method with ionization of neutrals accounted by Monte-Carlo technique [9]. The cross section of hydrogen ionization by electron impact is described by the fitting formula from [10]. Spatial distributions of the potential at each time step are obtained by solving of Poisson's equation with zero potential of the bulk plasma boundary, $\phi(-L) = 0$, and the field at the divertor plate, $E_w = -\sigma_w/\varepsilon_0$, where σ_w is the surface charge density of the plate. Typical time of calculations comes to a few thousands periods of the plasma ion oscillations until the steady state is achieved.

The real values of the system parameters for the simulation were chosen close to that of the divertor plasma: the temperatures of electrons and ions in the bulk plasma $T_{eb} = T_{ib} = 10\ eV$ and the density $n_b = 10^{12}\ cm^{-3}$. The length of the simulated system is $L = 100\lambda_D$, where $\lambda_D = (\varepsilon_0 T_{eb}/n_b e^2)^{1/2} = 23.5\ \mu m$ is the bulk electrons Debye length. With the purpose of getting the reliable presheath, whose length is order of ionization mean free path, fitted in the simulated system we effectively increased the neutral gas density that was $n_a = 10^{15}\ cm^{-3}$ with the temperature $T_a = 0.025\ eV$.

The huge difference in timescales of dust particles motion and plasma dynamics allows us to consider dynamics of a conducting spherical dust particle of radius R_d separately from formation of stationary plasma parameters in the system. To describe the motion of the dust particle in the divertor plasma we solve momentum and charging equations with the simulated plasma parameters:

$$m_d \frac{d^2x}{dt^2} = F(x,t), \quad \frac{dQ_d(x,t)}{dt} = I(x,t). \tag{1}$$

Here m_d is the mass of dust particle, Q_d is its charge, x is the position of dust particle, $F(x,t)$ and $I(x,t)$ are the local acting force and the flowing current onto the dust particle, respectively. The initial conditions for dust dynamics equations (1) imply the dust particle in contact with the divertor plate has zero velocity and electric charge that corresponds to the plates surface charge density:

$$x(t=0)=0, \quad \left.\frac{dx}{dt}\right|_{t=0}=0, \quad Q_d(t=0)=-4\pi\varepsilon_0 E_w R_d^2. \tag{2}$$

To calculate the local force and current onto the dust particle we need to know the local velocity distribution functions of electrons and ions. As the electron velocity distribution function, we assume Maxwellian distribution with the simulated local effective electron temperature $T_e(x)=m_e\left(\langle v_e^2\rangle-\langle v_e\rangle^2\right)|_x$, here brackets mean ensemble averaging, m_e is the mass of electron, v_e is local velocity of an electron. For ions, we assume the monoenergetic velocity distribution function with the simulated local ion flow velocity $V_i(x)$. These assumptions are good enough for the estimation purpose that will be confirmed in the next section by comparison of the estimated values of the plasma parameters based on the approximate functions with the simulated ones.

For a dust particle moving in the divertor plasma, we account the electrostatic force $F_E(x,t)=Q_d(x,t)E(x)$ and ion drag force due to the absorption of ions by dust particles $F_d(x,t)$, so that $F(x,t)=F_E(x,t)+F_d(x,t)$, where $E(x)$ is the local electric field. We neglected the drag forces concerned with electrons due to their small mass, and neutrals as frictional force that introduces only energy dissipation. Using the cross section for ion absorption by a spherical dust particle according to the orbital motion limited (OML) theory [11] and above assumption for the ion velocity distribution function the ion drag force acting on the dust particle can be written as

$$F_d(x,t)=\pi R_d^2 m_i n_i(x) V_i^2(x)\left(1-\frac{eQ_d(x,t)}{2\pi\varepsilon_0 R_d m_i V_i^2(x)}\right), \tag{3}$$

where m_i is the ion mass, $n_i(x)$ is the local ion density. The current on the dust particle consists of two components: electron current $I_e(x,t)$ and ion current $I_i(x,t)$. For the approximated distribution functions using the OML approach we can find

$$I_e(x,t)=-\pi R_d^2 e n_e(x)\sqrt{\frac{8T_e(x)}{\pi m_e}}\exp\left(\frac{eQ_d(x,t)}{4\pi\varepsilon_0 R_d T_e(x)}\right), \tag{4}$$

$$I_i(x,t)=\pi R_d^2 e n_i(x) V_i(x)\left(1-\frac{eQ_d(x,t)}{2\pi\varepsilon_0 R_d m_i V_i^2(x)}\right), \tag{5}$$

where $n_e(x)$ is the local density of electrons. Considering forces and currents on the dust particle, we have neglected dust particle velocity in comparison with electron and ion velocities owing to the large dust particle mass.

3 Distributions of plasma parameters

Simulated spatial distributions of the electric potential, the charge densities, the flow velocities and the effective temperatures of electrons and ions are shown in Fig. 1. We can see the

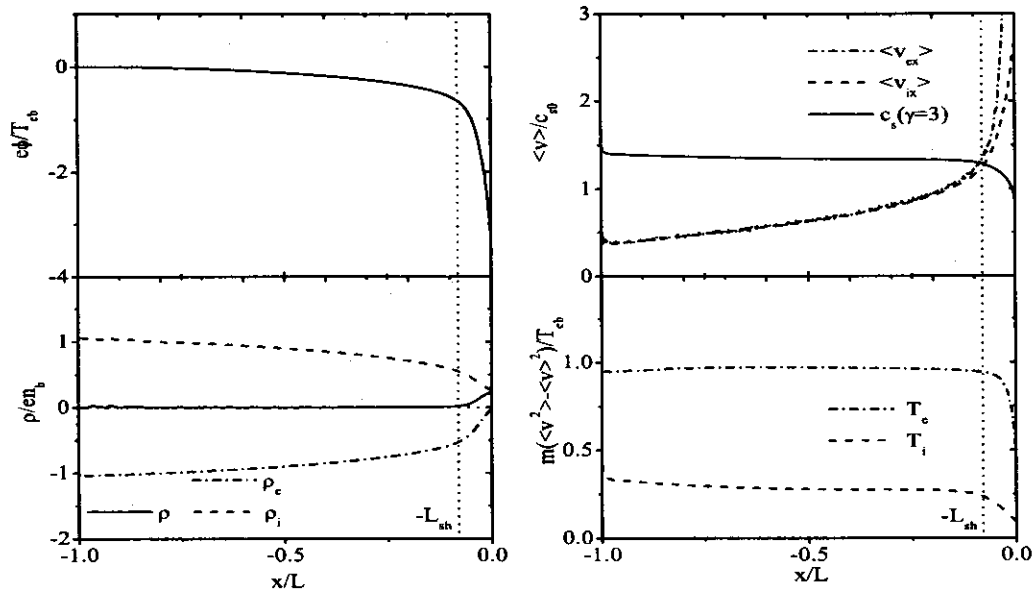

Fig. 1 Simulated spatial distributions of the electric potential, the charge densities, the flow velocities and the temperatures of plasma components in the system.

monotonic potential distribution in the system that includes the positively charged sheath and the quasineutral presheath. As expected the largest part of the potential drop between the floating plate and the bulk plasma falls on the sheath region. Inside the sheath, all parameters of the plasma change significantly due to rapid acceleration of ions and modification of the electron velocity distribution function. In contrast, inside the ionizing presheath region there is the weak electric field, the almost constant effective temperatures of electrons and ions, and gradual acceleration of ions toward the plate up to the sound speed accompanied with the density decreasing. According to the Bohm criterion we can define the sheath edge as the position, where the ion flow velocity equals to the local ion sound speed

$$c_s(x) = \left(\frac{T_e(x) + \gamma T_i(x)}{m_i} \right)^{\frac{1}{2}}, \tag{6}$$

for one dimensional adiabatic case constant $\gamma = 3$. The simulated spatial distribution of the ion sound speed is presented in Fig. 1 normalized by $c_{s0} = \sqrt{T_{eb}/m_i}$, where the obtained position of the sheath edge is indicated as $-L_{sh}$. The simulated value of L_{sh} is $5.4\lambda_{D,sh}$, where $\lambda_{D,sh} = 1.36\lambda_D$ is the obtained electron Debye length at the sheath edge.

To evaluate the results of plasma simulation we will compare the simulated potential drop on the sheath with that given by the theoretical estimation [12, 13]:

$$\phi_{sh} = \frac{1}{2}\frac{T_{e,sh}}{e} \ln\left(2\pi \frac{m_e c_{s,sh}^2}{T_{e,sh}} \right), \tag{7}$$

where $T_{e,sh}$ is electron temperature and $c_{s,sh}$ is the ion sound speed at the sheath edge. The simulated and estimated sheath potential drops, $e\phi_{sh}/T_{e,sh}$, are -2.74 and -2.56, respectively.

The estimated value was obtained with substitution of simulated parameters $c_{s,sh} = 1.28c_{s0}$ and $T_{e,sh} = 0.94T_{eb}$ in eq. (7).

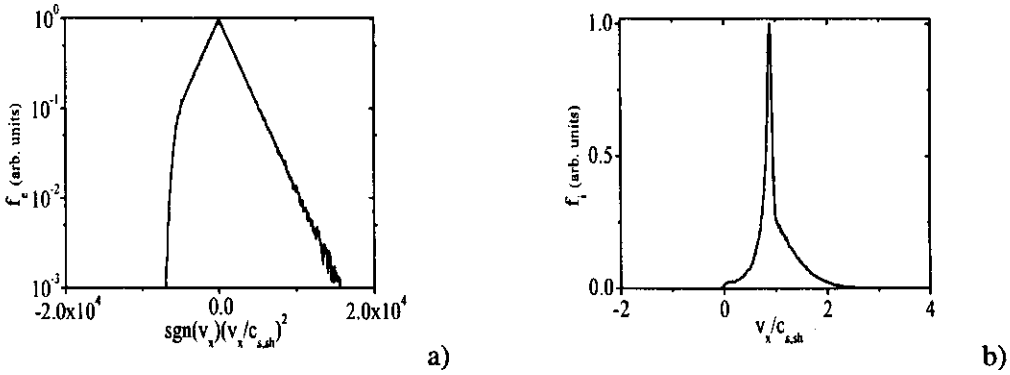

Fig. 2 The simulated velocity distribution functions of a) electrons and b) ions at the sheath edge.

The difference of the potential drops mainly is a consequence of assumptions that were made to get formula (7), the most important of which is the Maxwell-Boltzmann distribution for electrons. In a collisionless sheath, the supposition of Maxwellian electrons is not satisfied due to existence of electron current on the divertor plate. That means that part of high-energy electrons moving toward the plate is overcoming sheath potential and is absorbed by the plate, so that they do not return to the plasma to restore Maxwellian distribution. Therefore, high-energy negative velocity tail of the distribution function of electrons will be absent and their effective temperature and density are reduced. We can observe this effect in Fig. 2, where the simulated electron and ion distribution functions at the sheath edge are shown. Two groups of ions form presented ion velocity distribution function: injected from the bulk plasma and created by hydrogen ionization, both of which were accelerated by the presheath potential drop. Assuming that the slowest ions injected from the bulk plasma initially have zero velocity and are accelerated in the presheath, we can approximately find the part of the injected ions in the total ion density at the sheath edge. Such estimation shows that about half of the ions at the sheath edge was injected and correspondingly the other half was created by ionization. As can be seen, acceleration of the ions leads to narrowing of its velocity distribution function, that allows us to neglect their temperature as the first approximation, which was used to obtain the ion drag force and the current on dust particles.

4 Dust dynamics

Considering motion of dust particles started from the divertor plate we must at first answer the question — is it possible? Indeed, if the ion drag force exceeds the electrostatic force acting on a dust particle at the initial position on the divertor plate then it will never start to move. This condition can be written as $|F_d(x = 0)| > |F_E(x = 0)|$ for a dust particle of the given radius R_d. Substituting in this inequality the expressions for the forces and initial conditions (2), we can find that the dust particle can not leave the plate if its radius exceeds the critical

Table 1 The critical radius of dust particles calculated basing on estimated and simulated plasma parametes.

	$e\phi_{sh}/T_{e,sh}$	$n_{iw}/n_{e,sh}$	$v_{iw}/c_{s,sh}$	$e\lambda_{D,sh}E_w/T_{e,sh}$	$R_{c1}/\lambda_{D,sh}$
estimation	-2.56	0.46	2.03	0.62	3.0
simulation	-2.74	0.51	2.08	0.63	2.3

radius

$$R_{c1} = \frac{\varepsilon_0 |E_w|}{e n_{iw}} \left(2 - \frac{1}{\alpha}\right), \quad \alpha = \frac{2\varepsilon_0 E_w^2}{n_{iw} m_i V_{iw}^2}. \tag{8}$$

For the evaluation of this critical radius we can use the Bohm condition at the sheath edge together with the flux and energy conservation for ions under the assumption of their monoenergetic velocity distribution function. That gives us the following expressions for the ion density and the flow velocity at the position of the divertor plate $x = 0$:

$$\begin{aligned} n_{iw} &= n_b \frac{1 + M_b^2}{2} \left(1 - \frac{2e\phi_{sh}}{m_i c_{s,sh}}\right)^{-\frac{1}{2}}, \quad M_b = \frac{1}{\sqrt{2\pi}} \left(\frac{T_{eb}}{T_{ib}} + \gamma\right)^{-\frac{1}{2}}, \\ v_{iw} &= \left(c_{s,sh}^2 - \frac{2e\phi_{sh}}{m_i}\right)^{\frac{1}{2}}. \end{aligned} \tag{9}$$

Empirical estimation of the electric field at the divertor plate surface based on physically reasonable assumption that this field depends on the sheath potential drop and width gives

$$E_w = -\frac{\phi_{sh}}{4.1\lambda_{D,sh}}. \tag{10}$$

The calculated values of R_{c1} using the estimations (9) and (10) and simulated n_{iw}, v_{iw} and E_w are listed in Table 1. As can be seen, the critical dust radius is order of a few electron Debye lengths that is possible for dust in a not very rare plasma. It was evaluated the value of parameter α in eq. (8) is about unity, that conditioned by the floating plate potential. This means that changing of the plate potential with applied bias voltage it is possible to control the dust critical radius and probably to completely suppress the dust motion. The difference between estimated and simulated values in Table 1 is consequence of the simple monoenergetic ion approximation in eqs. (9), that also shows order of error made by such assumption.

For the following analysis of the dust motion in the simulated system, we obtained the equilibrium positions for a dust particle. If a dust particle with the given radius R_d is placed at some position in the plasma for sufficiently long time it obtains the local equilibrium charge $Q_{d,eq}(x)$, which corresponds to the total zero current on the dust particle $dQ_{d,eq}(x)/dt = 0$. If the local equilibrium charge of the dust particle at some position corresponds to the total zero force acting on it, then this position is equilibrium position x_{eq} of the dust particle of the radius R_d, so that $dx_{eq}/dt = 0$. Fig. 3 presents the calculated equilibrium positions and corresponding equilibrium charges for dust particles with the given radius R_d. Note that there

no equilibrium position exists for dust particles with the radius greater then R_{c2}^{cut} and there are two possible equilibrium positions for dust with the radius $R_{c2}^{cut} > R_d > R_{c2}^*$, where R_{c2}^* corresponds to the equilibrium position at the divertor plate $x_{eq} = 0$. If charging of the dust particle is much faster than changing of its position and the corresponding plasma parameters, then its charge $Q_d(x)$ and acting force $F(x)$ are functions of the dust position only. This situation can be realized for the heavy dust particles. That allows us to introduce the local effective potential energy of the dust particle $E_{eff}(x) = \int_0^x F(x')dx'$, Fig. 4. Minima of the effective potential energy correspond to the stable equilibrium positions of the dust particle and the maxima correspond to the unstable ones. According to Fig. 3 and 4, we can classify the motion of heavy dust particles started from the divertor plate on their radii:

$R_{c1} > R_d > R_{c2}^{cut}$ — There is no equilibrium position for the dust particle. The particle returns to the plate just after detachment from it, thus performing very short oscillations in immediate proximity to the divertor plate.

$R_{c2}^{cut} > R_d > R_{c2}^*$ — The dust particle initially placed at the plate cannot reach its equilibrium position due to existence of the effective potential energy barrier and returns to the plate. However, if the initial kinetic enegy of the dust particle is larger than this barrier it can oscillate around its equilibrium position.

$R_{c2}^* > R_d$ — There is only one equilibrium position for the dust particle that is the farther from the plate the smaller is the dust radius. The particle will oscillate around its equilibrium position.

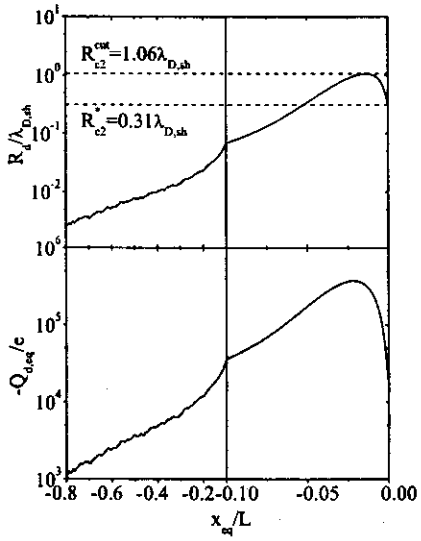

Fig. 3 The equilibrium positions and charges for dust particles of given radius.

Simulations of dynamics of the heavy dust particles with different radii using equations (1) and (2) allow us to obtain the maximal distances from the divertor plate that the dust particles can reach. Distributions of the maximal approaching distance on the dust radius in two systems

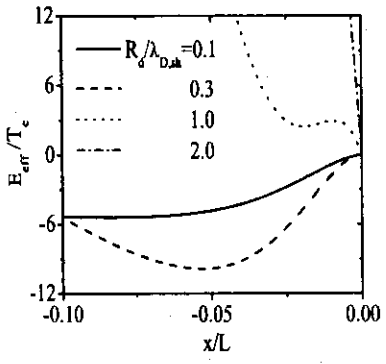

Fig. 4 Spatial distributions of the effective potential energy for dust particles with different radii.

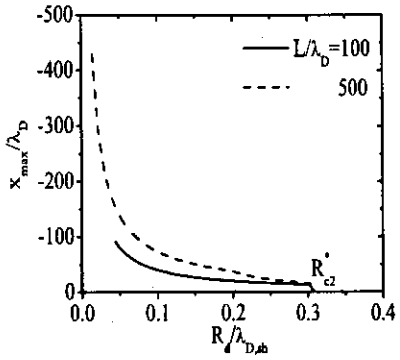

Fig. 5 The maximal distance from the plate that heavy dust particles approach in the systems of different lengths.

of different lengths are shown in the Fig. 5. As can be seen dust particles are capable to move away from the plate on significant distance only if their radius smaller than R^*_{c2}. The smaller is the dust the deeper it penetrates into plasma. Note also, that the maximal approaching distance for a dust particle located much farther from the plate than its equilibrium position, especially for small particles. Such small particles can reach the bulk plasma. Increasing of the presheath length leads to increasing of the maximal approaching distance for the dust with fixed radius, it contraries to the first glance that reducing of electric field in longer presheath will lead to decreasing of the maximal approaching distance. This result, however, shows that larger dust charge in longer presheath at the same distance from the plate makes electric force even stronger. As would be expected, the value of R^*_{c2} does not depend on presheath length as it is determined by conditions at the divertor plate.

5 Conclusion and remarks

The motion of heavy spherical dust particles in the divertor plasma was analyzed using solutions of dust dynamics equations. Corresponding spatial distributions of the divertor plasma parameters were obtained with PIC/MC computer simulations. It was shown that the critical dust radius exists, over which dust particles are incapable to move off the divertor plate due to larger ion drag force, and analytical expression for it was obtained. Changing of the plate potential, we can control the critical dust radius and there is possibility to suppress the dust motion from the plate. The classification of dust trajectories started from the divertor plate on dust radius was found: dust particles with the short range trajectories return to the plate without reaching the equilibrium positions, if theirs exist; other dust particles oscillate around their equilibrium positions. The maximal distance from the divertor plate that a dust particle can reach showed that the smaller dust could deeply penetrate into the SOL plasma and that the longer presheath increases the penetration depth.

Although we have analyzed dust motion in the simulated system, qualitative description of the motion is applicable to wide range of sheath-presheath systems due to common properties

of spatial potential distributions. The influence of truncated velocity distribution function of electrons and the effect of ion temperature on dust dynamics can be analyzed further, but probably will not change the phenomena qualitativly. Also additional forces on dust particles such as momentum transfer due to Coulomb collisions can be included in the consideration. It should be noted that here we examined the motions of heavy dust particles whose charge is equilibrium at any time. For the light dust that may not be the case and the effect of delayed dust charging can be important. This is one of our future issues. As the final target of the present research, we consider investigation of dust dynamics with distributed radii in self-consistent potential inside divertor plasmas.

References

[1] Yu. Chutov et.al., Phys. Plasmas **10**, 546–552 (2003).
[2] Y. Tomita et.al., Contrib. Plasma Phys. (this issue).
[3] J. Winter, Plasma Phys. Control Fusion **40**, 1201 (1998).
[4] J.P. Sharpe et.al., J. of Nucl. Materials **313–316**, 455–459 (2003).
[5] K-U. Riemann, J. Phys. D: Appl. Phys. **24**, 493–518 (1991).
[6] J.X. Ma et.al., Phys. Rev. E **55**, 4627 (1997).
[7] S.V. Vladimirov et.al., Phys. Plasmas **5**, 4 (1998).
[8] S.V. Vladimirov and N.F. Cramer, Phys. Rev E **62**, 2754–2762 (2000).
[9] C.K. Birdsall, IEEE Trans. Plasma Sci. **19**(2), 65–85 (1991).
[10] W. Lotz, Electron Impact ionization Cross-Sections and Ionization Rate Coefficients for Atoms and Ions from Hydrogen to Calcium, Tech. Rep., Institut für Plasmaphysik, Garching bei München (1967).
[11] J.E. Allen, Physica Scripta **45**, 497–503 (1992).
[12] M.A. Lieberman and A.J. Lichtenberg, Principles of Plasma Discharges and Materials Processing (John Wiley & Sons, New York, 1994), chap. 6, pp. 154–171.
[13] P.C. Stangeby, The Plasma Boundary of Magnetic Fusion Devices (Institute of Physics Pub., Bristol and Philadelphia, 2000), chap. 2, pp. 61–105.

Recent Issues of NIFS Series

NIFS-761 K. Yamazaki, S. Imagawa, T. Muroga, A. Sagara, S. Okamura
System Assessment of Helical Reactors in Comparison with Tokamaks
Oct. 2002 (FT/P1-20)

NIFS-762 S. Okamura, K. Matsuoka, S. Nishimura, M. Isobe, C. Suzuki, A. Shimizu, K. Ida, A. Fujisawa, S. Murakami, M. Yokoyama, K. Itoh, T. Hayashi, N. Nakajima, H. Sugama, M. Wakatani, Y. Nakamura, W. Anthony Cooper
Physics Design of Quasi-Axisymmetric Stellarator CHS-qa
Oct. 2002 (IC/P-07)

NIFS-763 Lj. Nikolic, M.M. Skoric, S. Ishiguro and T. Sato
On Stimulated Scattering of Laser Light in Inertial Fusion Energy Targets
Nov. 2002

NIFS-764
NIFS Contributions to 19th IAEA Fusion Energy Conference (Lyon, France, 14-19 October 2002)
Nov. 2002

NIFS-765 S. Goto and S. Kida
Enhanced Stretching of Material Lines by Antiparallel Vortex Pairs in Turbulence
Dec. 2002

NIFS-766 M. Okamoto, A.A. Maluckov, S. Satake, N. Nakajima and H. Sugama
Transport and Radial Electric Field in Torus Plasmas
Dec. 2002

NIFS-767 R. Kanno, N. Nakajima, M. Okamoto and T. Hayashi
Computational Study of Three Dimensional MHD Equilibrium with m/n=1/1 Island
Dec. 2002

NIFS-768 M. Yagi, S.-I. Itoh, M. Kawasaki, K. Itoh and A. Fukuyama
Multiple-Scale Turbulence and Bifurcaion
Jan. 2003

NIFS-769 S.-I. Itoh, K. Itoh and S. Toda
Statistical Theory of L-H Transition and its Implication to Threshold Database
Jan. 2003

NIFS-770 K. Itoh
Summary: Theory of Magnetic Confinement
Jan. 2003

NIFS-771 S.-I. Itoh, K. Itoh and S. Toda
Statistical Theory of L-H Transition in Tokamaks
Jan. 2003

NIFS-772 M. Stepic, L. Hadzievski and M.M. Skoric
Modulation Instability in Two-dimensional Nonlinear Schrodinger Lattice Models with Dispersion and Long-range Interactions
Jan. 2003

NIFS-773 M.Yu. Isaev, K.Y. Watanabe, M. Yokoyama and K. Yamazaki
The Effect of Hexapole and Vertical Fields on α-particle Confinement in Heliotron Configurations
Mar. 2003

NIFS-774 K. Itoh, S.-I. Itoh, F. Spineanu, M.O. Vlad and M. Kawasaki
On Transition in Plasma Turbulence with Multiple Scale Lengths
May 2003

NIFS-775 M. Vlad, F. Spineanu, K. Itoh, S.-I. Itoh
Intermittent and Global Transitions in Plasma Turbulence
July 2003

NIFS-776 Y. Kondoh, M. Kondo, K. Shimoda, T. Takahashi and K. Osuga
Innovative Direct Energy Conversion Systems from Fusion Output Thermal Power to the Electrical One with the Use of Electronic Adiabatic Processes of Electron Fluid in Solid Conductors.
July 2003

NIFS-777 S.-I. Itoh, K. Itoh and M. Yagi
A Novel Turbulence Trigger for Neoclassical Tearing Modes in Tokamaks
July 2003

NIFS-778 T. Utsumi, J. Koga, T. Yabe, Y. Ogata, E. Matsunaga, T. Aoki and M. Sekine
Basis Set Approach in the Constrained Interpolation Profile Method
July 2003

NIFS-779 Oleg I. Tolstikhin and C. Namba
CTBC A Program to Solve the Collinear Three-Body Coulomb Problem: Bound States and Scattering Below the Three-Body Disintegration Threshold
Aug. 2003

NIFS-780
Contributions to 30th European Physical Society Conference
on Controlled Fusion and Plasma Physics
(St.Petersburg, Russia, 7-11 July 2003)
from NIFS
Aug. 2003

NIFS-781 Ya. I. Kolesnichenko, K. Yamazaki, S. Yamamoto, V.V. Lutsenko, N. Nakajima, Y. Narushima, K. Toi, Yu. V. Yakovenko
Interplay of Energetic Ions and Alfvén Modes in Helical Plasmas
Aug. 2003

NIFS-782 S.-I. Itoh, K. Itoh and M. Yagi
Turbulence Trigger for Neoclassical Tearing Modes in Tokamaks
Sep. 2003

NIFS-783 F. Spineanu, M. Vlad, K. Itoh, H. Sanuki and S.-I. Itoh
Pole Dynamics for the Flierl-Petviashvili Equation and Zonal Flow
Sep. 2003

NIFS-784 R. Smirnov, Y. Tomita, T. Takizuka, A. Takayama, Yu. Chutov
Particle Simulation Study of Dust Particle Dynamics in Sheaths
Oct. 2003